Electrical resistivity structure at the SAFOD site from magnetotelluric exploration

Martyn Unsworth
Institute for Geophysical Research, Department of Physics, University of Alberta, Edmonton, Alberta, Canada

Paul A. Bedrosian
GeoForschungsZentrum, Potsdam, Germany

Received 31 December 2003; revised 6 February 2004; accepted 13 February 2004; published 18 May 2004.

[1] The magnetotelluric dataset collected on the San Andreas Fault at Parkfield has been re-analyzed using superior inversion algorithms that have been developed in recent years. A combination of constrained inversion, forward modeling and synthetic inversion studies are used, and show that at the SAFOD site, the low resistivity fault zone extends to a depth of 2–3 km. An extended zone of low resistivity east of the San Andreas Fault may be connected to the SAF at seismogenic depths. The connection increases along the SAF to the northwest and may be related to the transition from locked to creeping seismic behavior. *INDEX TERMS:* 7209 Seismology: Earthquake dynamics and mechanics; 7230 Seismology: Seismicity and seismotectonics; 8010 Structural Geology: Fractures and faults; 8123 Tectonophysics: Dynamics, seismotectonics. **Citation:** Unsworth, M., and P. A. Bedrosian (2004), Electrical resistivity structure at the SAFOD site from magnetotelluric exploration, *Geophys. Res. Lett.*, *31*, L12S05, doi:10.1029/2003GL019405.

1. Introduction

[2] The San Andreas Fault (SAF) at Parkfield is one of most accessible locations at which the mechanics of strike-slip faulting and the associated earthquake cycle can be studied. Prior to the drilling of the SAFOD well, geophysical imaging has been extensively used to image the structure of the fault from the surface. Remote sensing of subsurface electrical resistivity has been achieved using the magnetotelluric (MT) method. Three profiles were collected in 1994 and 1997 on Middle Mountain. An initial analysis of these data was presented in *Unsworth et al.* [1997, 2000] and revealed a wedge of low resistivity west of the San Andreas Fault. This feature was interpreted as a zone of fractured rock and termed the fault-zone conductor, or FZC. This discovery played a crucial role in locating the SAFOD well to the west of the fault where less fractured bedrock is found. The MT method produces a resistivity image of the subsurface using low-frequency electromagnetic waves that diffuse in the earth. This gives a resolution comparable to seismic tomography, but lower than seismic reflection surveys. However, in an environment with highly fractured rock, MT can image structure in zones where seismic reflection produces incoherent reflections. In this paper a rigorous analysis of the MT data is presented. The goal is to understand the resolution of the MT data, and the degree to which the resistivity models are required by the data. This includes application of new inversion methods, hypothesis testing through constrained inversion and synthetic inversion studies.

0094-8276/04/2003GL019405$05.00

2. Magnetotelluric Data Analysis

[3] The data analysis began with the combined dataset from the 1994 and 1997 MT surveys. The data consist of continuous MT profiles with 100 m station spacing, and widely spaced stations to constrain regional structure. The MT data were grouped into three profiles (Figure 1) and inverted using the algorithm of *Rodi and Mackie* [2001]. The inversions used all available data, including the transverse electric (TE) mode, transverse magnetic (TM) mode and vertical magnetic field transfer functions (T_{yz}) in the frequency band 100–0.001 Hz. Previous inversions did not include the magnetic field transfer functions. This inversion algorithm produces a model that fits the data while satisfying a range of regularization criteria. In this study, the models were required to be spatially smooth, but the model was not required to be close to the starting model. Multiple inversions were performed to establish the degree to which these three subsets of data are mutually consistent. Representative models for Lines 1 and 3 are shown in Figure 2. Note that Line 0 is not shown in Figure 2. Vertical magnetic field data were not collected on this profile, and this, combined with larger standard errors, made objective comparison of the three profiles difficult. The models exhibit most features presented in earlier analyses of this data set. This includes the contrast of the resistive Salinian granite to the west of the San Andreas Fault, and the relatively low resistivity of the Great Valley sequence and Franciscan formation to the east. The models show the fault-zone conductor (FZC) bounded on the east side by the SAF trace and extending to a depth of 2–3 km. Figure 3 shows the fit of the recorded data in terms of pseudosections. This is a plot of data misfit normalized by the standard error of each datum.

[4] To evaluate if features in the model are required by the data, a hypothesis testing approach was used. In the initial step, the model for Line 1 was perturbed so that the FZC terminated at 1 km. The forward response of this model was computed and the predicted TE mode phase at a station west of the SAF is shown in Figure 4a. It is clear that a shallow (1 km) conductor is inconsistent with the MT data, and the increased fault-zone resistivity produces a

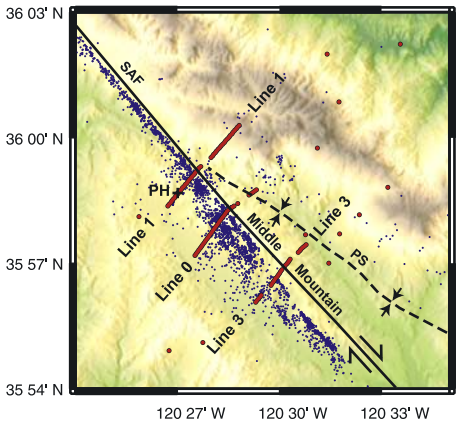

Figure 1. Location of the MT stations in the Parkfield area (red circles). The blue dots denote earthquakes from *Thurber et al.* [2003, 2004] and the High Resolution Seismic Network catalog [*Nadeau and McEvilly*, 1997]. PH = SAFOD pilot hole. PS = Parkfield Syncline. SAF = San Andreas Fault.

lower phase than observed between 3–0.3 Hz. However, this forward modeling exercise is a necessary, but not sufficient, condition for proving that the FZC does not terminate at 1 km. The non-uniqueness inherent in MT data make it possible that changing other parts of the model could also result in a statistically acceptable data misfit. To evaluate this possibility, constrained inversion was used, in which the inversion was restarted from the perturbed model, with the perturbed region fixed. MT data usually determine the conductance of a buried layer (product of thickness and conductivity). Thus several models with the same conductance, but differing thickness can all fit the same data, a phenomena termed equivalence. This is observed in the

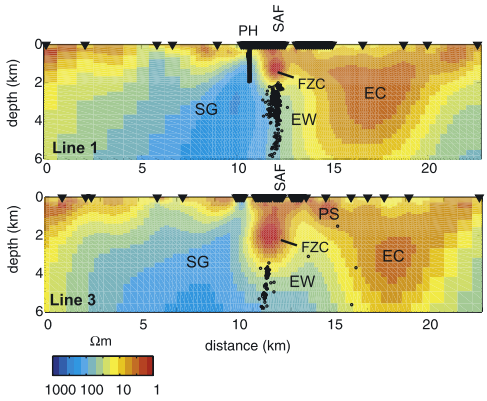

Figure 2. Resistivity models for Lines 1 and 3 from inversion of TE, TM and vertical magnetic field data. In each inversion error floors were applied (ρ_{TM} 10%, ρ_{TE} 20%, phase 5%, T_{zy} 0.02). The final root mean squared misfits are 1.80 (Line 1) and 2.05 (Line 3). The larger error floors on apparent resistivity allow the estimation of static shift coefficients. These were generally found to be in the range 1.2 to 0.8. SAF = San Andreas Fault surface trace, PH = SAFOD Pilot Hole, PS = Parkfield syncline, SG = Salinian Granite, EC = Eastern conductor, EW = East Wall of San Andreas Fault, FZC = Fault zone conductor. In both models VE = 1:1.

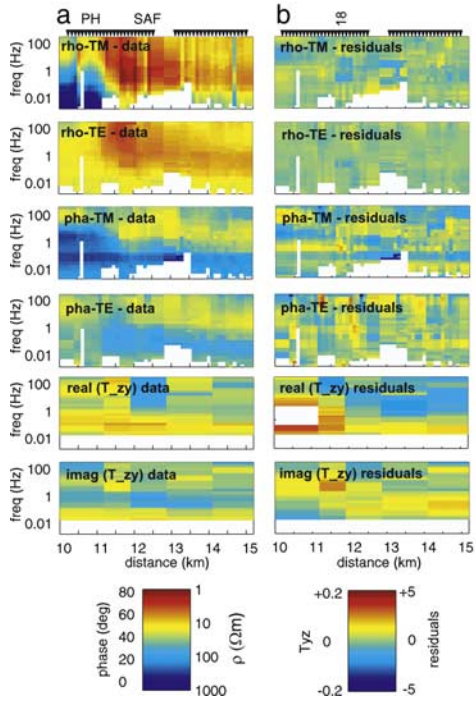

Figure 3. (a) Measured data for Line 1 in pseudosection format. (b) Misfit for the Line 1 model in Figure 2, shown normalized residuals. The residuals are the data misfit divided by the standard error for that datum, and the same residual scale is used for all data. Most data are fit within ±1 residual.

constrained inversion, as the algorithm attempts to fit the MT data by lowering the resistivity in the FZC between the surface and 1 km depth. However, this is only partially successful for a surface layer, where the MT data directly constrain the resistivity of the layer. The constrained inversion converged and the new response is shown in Figure 4a. The original fit is not recovered, indicating that the surface resistivity is too low. A similar test was also performed with the entire model fixed, except for the FZC from the surface to 1 km depth and similar results were obtained. We thus conclude that a model with a 1km deep FZC is incompatible with the data. The same response was observed at multiple stations west of the San Andreas Fault, and illustrates the value of the continuous MT profiling approach that allows for spatial redundancy in the measured MT data.

[5] Similar tests were undertaken for a model with the FZC extended to 5 km as shown in Figure 4b. This model increases the TE phase in the frequency band 1–0.1 Hz. When the constrained inversion is performed, the original fit is almost regained, with the fault zone having a higher resistivity, as expected from equivalence. The model was also more resistive to the west of the fault (4–6 km offset). This shows that there is some ambiguity in the inversion, since the TE mode cannot easily distinguish between a deeper fault zone conductor and a conductor to the west. This is largely due to the non-uniform station layout.

[6] As an additional test of resolution, a series of synthetic inversions were performed. Synthetic data were computed for a range of models, including those shown in Figure 5. Realistic noise was added and the data inverted

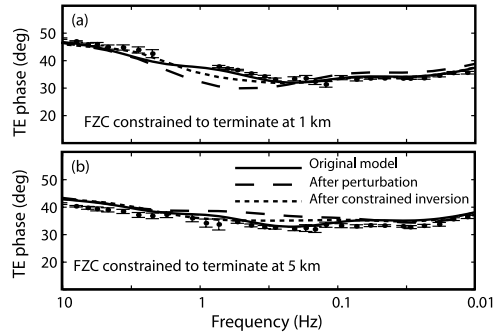

Figure 4. (a) TE mode phase response at station 18 on Line 1 west of the San Andreas Fault, illustrating the constrained inversion. This is the 18th station in the continuous array. The FZC was terminated at 1 km, producing a lower phase than observed. After restarting the inversion with the perturbed area fixed, the original fit was not regained. (b) Same responses when the FZC is extended to 5 km depth.

with identical parameters to those used in the inversion of the field data. The inversion models show that the depth of the FZC can be well resolved. The synthetic inversions reveal that some artifacts arise due to the finite length of the continuous MT profile and the rapid increase in spacing at each end of the profile. One such artifact is the westward dip of the top of the Salinian granite, which is also present in the inversion of field data (Figure 2). The synthetic inversions also show that the vertical contact below the FZC is not recovered. Rather, the resistivity is imaged as a smooth horizontal transition. This indicates that in the real inversion models (Figure 2), the resistivity of the Franciscan formation east of the SAF is an upper bound. As a final test of the inversion models, they have been compared with resistivity log data from the SAFOD pilot hole. The agreement is reasonable, as further described by *Boness and Zoback* [2004]. The MT models also agrees well with the velocity models of *Thurber et al.* [2003, 2004].

3. Interpretation

[7] Having established the reliability of the inversion models, it is important to consider the implications for fault zone structure. It is clear that the FZC extends to a depth of at least 2 km on Line 1, and possibly deeper. On Line 3, the FZC extends to 3 km, and similar constrained inversions indicate this depth is well determined. Earthquake hypocenters indicate a near vertical San Andreas Fault that bounds the east side of the FZC [*Thurber et al.*, 2004]. The onset of micro earthquakes at the base of the FZC may reflect the depth at which fault rocks have become strong enough to accumulate sufficient stress for brittle failure to occur. The low resistivity of the FZC is primarily due to the low resistivity fluid in the pore space. Porosity estimates in the range 8–30% were calculated by *Unsworth et al.* [1997, 2000]. The MT data cannot, however, determine the lithology of the fractured rock, since the low resistivity primarily reflects the pore fluid, rather than the rock itself. These fluids may or may not be involved in the earthquake cycle at Parkfield. Their significance in the shallow fault is that they impart a low resistivity to a fractured, saturated rock. Variations in the depth of the FZC are the result changes in the fracture density, fluid composition, and fluid concentration.

[8] *Park and Roberts* [2003] proposed an alternative explanation for the FZC and suggested that it is in fact the Parkfield syncline, a shallow feature striking sub-parallel to the SAF and located to the southeast of the SAFOD site. While this idea is plausible, it is inconsistent with the MT data set for several reasons:

[9] (1) When all three Middle Mountain profiles are considered it is clear that the FZC is not the Parkfield syncline. Line 3 images both the Parkfield syncline and the FZC [*Unsworth et al.*, 2000] (Figure 2). These features are superimposed on Line 1 [*Dibblee et al.*, 1999]. On Line 0 the Parkfield syncline is located at the end of the profile where resolution is low [*Unsworth et al.*, 1997]. Thus it is not surprising it was not imaged on Line 0.

[10] (2) A very similar FZC is observed at Hollister [*Bedrosian et al.*, 2002] and appears to be typical of large parts of the creeping San Andreas Fault, rather than an anomaly of the local geology at Parkfield.

[11] (3) It should also be noted that the microearthquake locations shown in *Unsworth et al.* [1997] were west of the surface trace. Subsequent seismic surveys have shown they are actually located beneath the surface trace [*Thurber et al.*, 2004], which confirms that the SAF trace in on the east side of the FZC. The incorrect location of these events was suggested by *Park and Roberts* [2003] as evidence that the FZC was unrelated to the San Andreas Fault.

[12] The deeper zone of low resistivity east of the SAF may represent a major source of crustal fluids. This feature (EC) exhibits resistivity values around 3 Ωm. The geology east of the SAF comprises both Great Valley sequence and Franciscan formation, and layers of serpentinite may act as seals, creating an underlying zone of over pressured fluid [*Dibblee et al.*, 1999; *McPhee et al.*, 2004]. On Line 1, geological and potential field data show that a layer of serpentinite may be located at 2 km depth. The resistivity model in Figure 2 shows a decrease in resistivity at about 1 km depth. Sensitivity tests show that this depth is well constrained by the MT data. Thus the potential field and MT data might be reconciled by noting the non-uniqueness in the potential field data, or the presence of multiple zones of saline groundwater in this area. Serpentinite can exhibit a low resistivity [*Palacky*, 1991] and thus the low resistivity of EC could be due to both a serpentinite layer and the

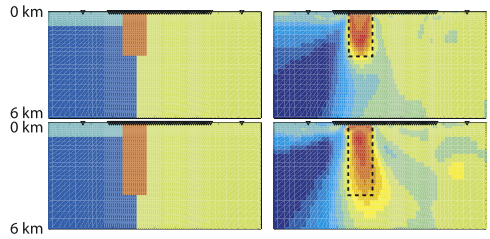

Figure 5. Synthetic inversion study of depth of FZC. Left column shows two models from which synthetic data were computed. After noise was added, the TE, TM and vertical magnetic field data were inverted to produce the models in the right column. VE = 1:1. Colour scale is the same as in Figure 2. Dashed lines indicates true extent of the FZC.

underlying saline aquifer. However other studies suggest that serpentinite may not exhibit such a low resistivity (F. Schilling, personal communication, 2004). In addition to lowering the electrical resistivity, these fluids produce a coincident low velocity zone with similar geometry and depth extent [*Thurber et al.*, 2004].

[13] Is there evidence for pathways from this fluid zone (EC) into the SAF at seismogenic depths? At first impression Figure 2 suggests that the low resistivity does not extend to the east wall (EW) of the SAF at depth and that fluids are confined to a synclinal structure 2–3 km east of the SAF. However, this is not the case, since at a depth of 5 km the resistivity in the east wall (EW) of the San Andreas Fault is around 30 Ωm. Assuming a pore fluid salinity of 30,000 ppm (as observed in the nearby Varian well), this implies a porosity of 1–10% [*Archie*, 1942]. Note also that the synthetic inversions show this is an upper bound on the resistivity, which could be significantly lower. This in turn corresponds to a lower bound on porosity. In absolute terms, the porosity in the east wall is quite high and it is likely that fluids and entering the fault zone from the east.

4. Conclusions

[14] The sensitivity analysis of the MT data presented here has shown that previous interpretations are well supported by the MT data. The wedge of broken rock that produces the characteristic FZC has a variable, but well constrained depth extent of 2–3 km. The connection of aquifers in the Franciscan formation increases to the northwest, as the fault begins to creep. Additional data are still needed to fully understand the influence of crustal fluids on the seismic behavior of the San Andreas Fault at this location. Additional MT data away from the fault would reveal if the locked to creeping transition is truly controlled by connection to the Franciscan aquifers, as suggested by *Irwin and Barnes* [1974]. Well log resistivity measurements in the main SAFOD well will also reveal the nature of fluids that are present in the fault zone at 4 km depth, below the FZC.

[15] **Acknowledgments.** MT data collection was funded by NSF (grant EAR9614411), the U.S. Geological Survey (grants 1434-HQ-97-GR-03157 and 1434-HQ-97-GR-03152) and the U.S. Department of Energy (grant DE EG03-97ER-14871). Data analysis was supported by research grants from NSERC and the University of Alberta. We thank Randy Mackie for the use of his inversion algorithm, and Parkfield landowners for access to their property. Ersan Turkoglu and Volkan Tuncer assisted with map production. Comments by anonymous reviewers are gratefully acknowledged.

References

Archie, G. E. (1942), The electrical resistivity log as an aid in determining some reservoir characteristics, *Trans. Am. Inst. Min. Metall. Pet. Eng.*, *146*, 54–62.

Bedrosian, P. A., M. J. Unsworth, and G. D. Egbert (2002), Magnetotelluric imaging of the creeping segment of the San Andreas Fault near Hollister, *Geophys. Res. Lett.*, *29*, 1506, doi:10.1029/2001GL012119.

Boness, N. L., and M. D. Zoback (2004), Stress-induced seismic velocity anisotropy and physical properties in the SAFOD Pilot Hole in Parkfield, CA, *Geophys. Res. Lett.*, *31*, L13S17, doi:10.1029/2003GL019020, in press.

Dibblee, T. W., S. E. Graham, T. M. Mahony, J. L. Blissenbach, J. J. Mariant, and C. M. Wentworth (1999), Regional geologic map of San Andreas and related faults in Carrizo Plain, Temblor, Caliente and La Panza Ranges and vicinity, California: A digital database, *U. S. Geol. Surv. Open File Rep. 99-14*, scale 1:125,000.

Irwin, W., and I. Barnes (1974), Effect of geologic structure and metamorphic fluids on seismic behavior of the San Andreas fault system in central and northern California, *Geology*, *3*, 713–716.

McPhee, D., R. C. Jachens, and C. M. Wentworth (2004), Crustal structure of the San Andreas Fault at the SAFOD site from potential field and geologic studies, *Geophys. Res. Lett.*, *31*, L12S03, doi:10.1029/2003GL019363.

Nadeau, R., and T. V. McEvilly (1997), Seismological studies at Parkfield V: Microearthquake sequences as fault-zone drilling targets, *Bull. Seismol. Soc. Am.*, *87*, 1463–1472.

Palacky, G. J. (1991), Resistivity characteristics of geologic targets, in *Electromagnetic Methods in Applied Geophysics*, edited by M. Naibighian, pp. 53–129, Soc. of Explor. Geophys., Tulsa, Okla.

Park, S. K., and J. J. Roberts (2003), Conductivity structure of the San Andreas fault, Parkfield, revisited, *Geophys. Res. Lett.*, *30*(16), 1842, doi:10.1029/2003GL017689.

Rodi, W., and R. L. Mackie (2001), Nonlinear conjugate gradients algorithm for 2-D magnetotelluric inversion, *Geophysics*, *66*, 174–187.

Thurber, C., S. Roecker, K. Roberts, M. Gold, L. Powell, and K. Rittger (2003), Earthquake locations and three-dimensional fault zone structure along the creeping section of the San Andreas fault near Parkfield, CA: Preparing for SAFOD, *Geophys. Res. Lett.*, *30*(3), 1112, doi:10.1029/2002GL016004.

Thurber, C., S. Roecker, H. Zhang, S. Baher, and W. Ellsworth (2004), Fine-scale structure of the San Andreas fault zone and location of the SAFOD target earthquakes, *Geophys. Res. Lett.*, *31*, L12S02, doi:10.1029/2003GL019398.

Unsworth, M. J., P. E. Malin, G. D. Egbert, and J. R. Booker (1997), Internal structure of the San Andreas fault zone at Parkfield, California, *Geology*, *25*, 359–362.

Unsworth, M. J., M. Eisel, G. D. Egbert, W. Siripunarvaporn, and P. A. Bedrosian (2000), Along-strike variations in the structure of the San Andreas fault at Parkfield, California, *Geophys. Res. Lett.*, *27*, 3021–3024.

P. A. Bedrosian, GeoForschungsZentrum, Telegrafenberg, D-14473 Potsdam, Germany. (bedros@gfz-potsdam.de)

M. J. Unsworth, Institute for Geophysical Research, Department of Physics, University of Alberta, Edmonton, Alberta T6G 2J1, Canada. (unsworth@phys.ualberta.ca)